# *Appendix 1*

## *Section 1* *Experimental Results on Stress-Strain Relation of Ti-Ni Shape Memory Alloy Bars and Their Application to Seismic Control of Buildings*

*presented by T. Fukuta*

# Experimental Results on Stress-Strain Relation of Ti-Ni Shape Memory Alloy Bars and their Application to Seismic Control of Buildings

**Toshibumi Fukuta[1] & Masanori Iiba[2]**

[1] *International Institute of Seismology & Earthquake Engineering, Building Research Institute, Tsukuba, Japan*
[2] *Department of Structural Engineering, Building Research Institute, Tsukuba, Japan.*

**ABSTRACT**

The mechanical property of Ti-Ni shape memory alloy (SMA) for tension and compression was investigated under super-elasticity. The test results demonstrated that the stress-strain curve for compressive stress is completely different from that for tensile stress, irrespective of whether the load is static or dynamic in nature. Super-elasticity was clearly evident under tensile strain of up to around 5%, but not under compressive strain, due to residual strain. Based on these results, SMA bars were examined to apply to the brace-type response-control devices for houses in their super-elasticity phase. It was found out that SMA has an effect to restore lateral drift of the structures to zero.

## 1. INTRODUCTION

SMA is a unique material that, when subject to stress, exhibits a “memory shape” effect linked to temperature and also undergoes changes in basic properties such as super-elasticity. These characteristics could potentially be applied to buildings to allow a degree of control over the building’s behavior in response to external forces, opening up new possibilities in building design. Although the tensile characteristics of thin wire have already been reported in experiments on the stress-strain relationship, temperature change, and strain rate under super-elastic conditions, little is known about how SMA behaves when subjected to compression. This study was designed to determine experimentally the stress-strain relationship in SMA bars in super-elastic alloy phase when subjected to compressive and tensile forces. Based on these results, SMA device of brace type response control for houses was examined by analysis.

## 2. Stress Strain Relation of SMA Bar

The alloy composition (Ti-Ni-Co alloy) and manufacturing conditions were carefully selected so that the test specimen would exhibit super-elastic properties at room temperature. Figure 1 schematically shows material phase and transformation temperatures as measured using a differential scanning calorimeter. The specimen with diameter 7 mm was fabricated from a bar of diameter 17 mm (Figure 2). The ambient temperature was around 26° C during the experiment. The readings from the two facing strain gauges were monitored to watch whether the test piece was centrally loaded. The readings deviated from one another only very slightly during the experiment. Similarly, eccentricity under the compression load did not reach significant levels. The load waveform used a triangular displacement-time relationship for both static and dynamic loads.

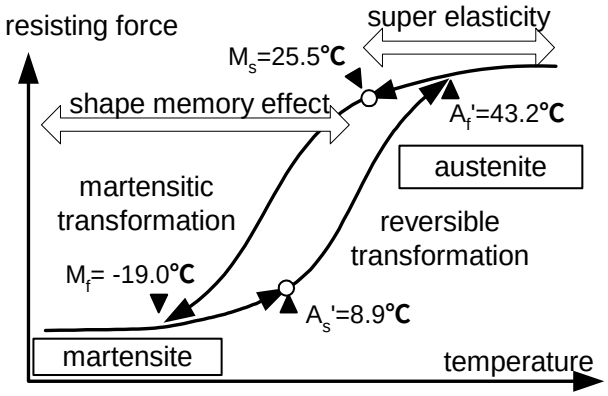


**Figure 1.** Transformation temperature & material phase

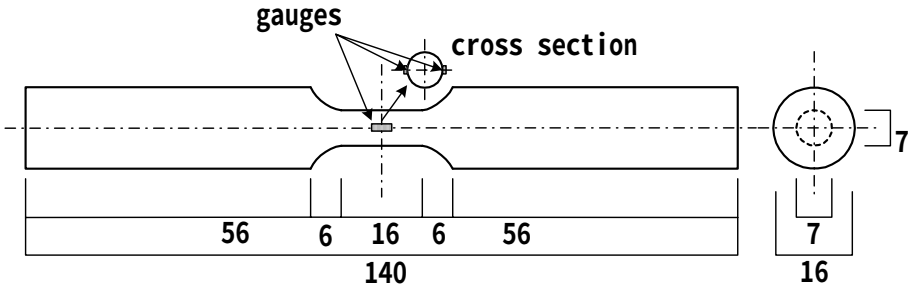


**Figure 2.** Test specimen

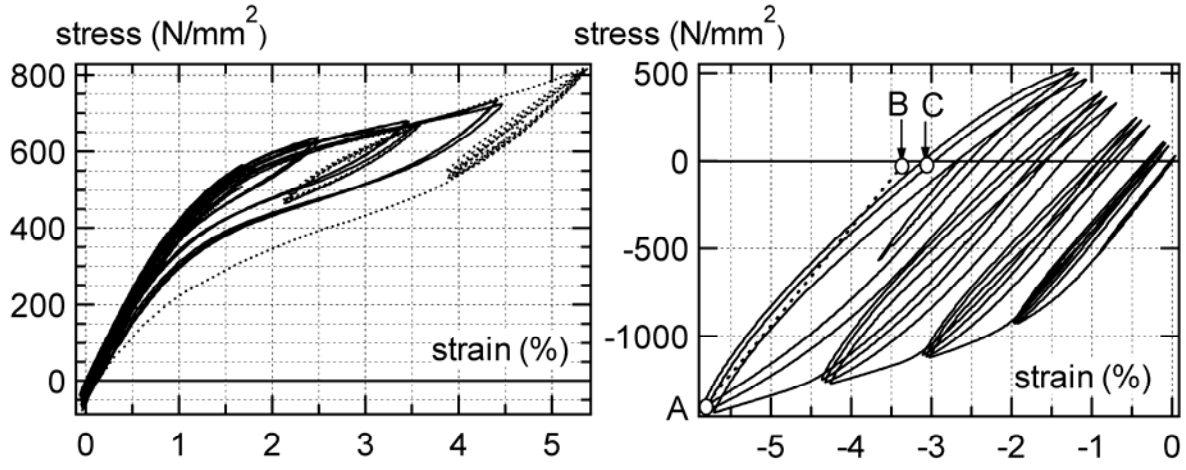


**a)** in tension **b)** in compression

**Figure 3.** Comparison of Stress-strain curves for tension test and compressive one

Figure 3-a) shows the stress-strain relationship for the static tensile test. The experiment began with three repetitions at each level (0%–1%, 0% –2%, etc.), as shown by the solid line. The specimen was then placed in a hot water bath at 50° C (hotter than the temperature at the end of the reverse transformation) for ten minutes, and repetitions were performed during unloading (at 0% – 2%, 2% –

4%, etc.). The strain generally returned to zero after each loading, clearly indicating super-elastic properties. Strain hardening can be observed from around 4% strain, where the curve gradient starts increasing. A very small amount of residual strain was observed after removal of the strain (approximately 4.5%).

Figure 3-b) shows the stress-strain curve under compression. Since the load was controlled by the distance between the two chucks of the loading machine, the paths of the stress-strain curve took were not exactly the same for all the sets of tests, because of the residual strain that remained in the test piece after removal of the load. The curve for compression forces differs in shape from the tension curve in Figure 3-a). The strain value shows no sign of the super-elasticity which would cause it to revert to zero upon removal of the load. The residual strain in fact resembles the stress-strain relationship for cold-formed carbon steel. Line AB is parallel to the initial stiffness, then strain BC shows a strain reversion.

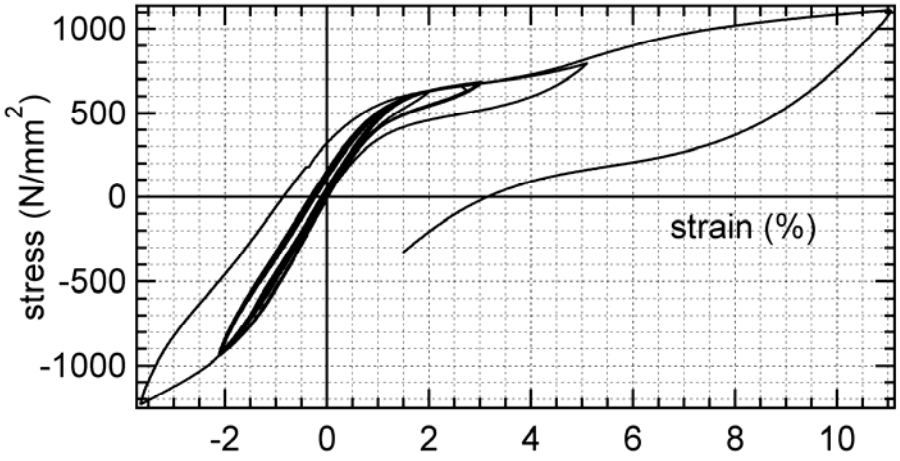


**Figure 4.** Stress-strain relationship for static tensile-compressive tests

Figure 4 shows the results of the tensile-compressive tests. The stress-strain relationship differs in many respects (yield strength, rigidity of plateau area after yielding, final strain value after removal of load) between the tension and the compression tests. Residual strain was observed after compression, but this could be negated almost completely by then applying a tensile strain that was greater (in absolute terms) than the compression strain that caused the residue.

**Table 1.** Average strain rate

| strain amplitude | 1st 10 cycles | 2nd 10 cycles | 3rd 10 cycles | 4th 10 cycles |
|---|---|---|---|---|
| ±1% | 0.828 | 3.89 | 16.5 | - |
| ±2% | 0.798 | 3.90 | 16.5 | 27.1 |
| ±4% | 0.973 | 4.69 | 21.5 | 37.1 |

Unit : %/sec.

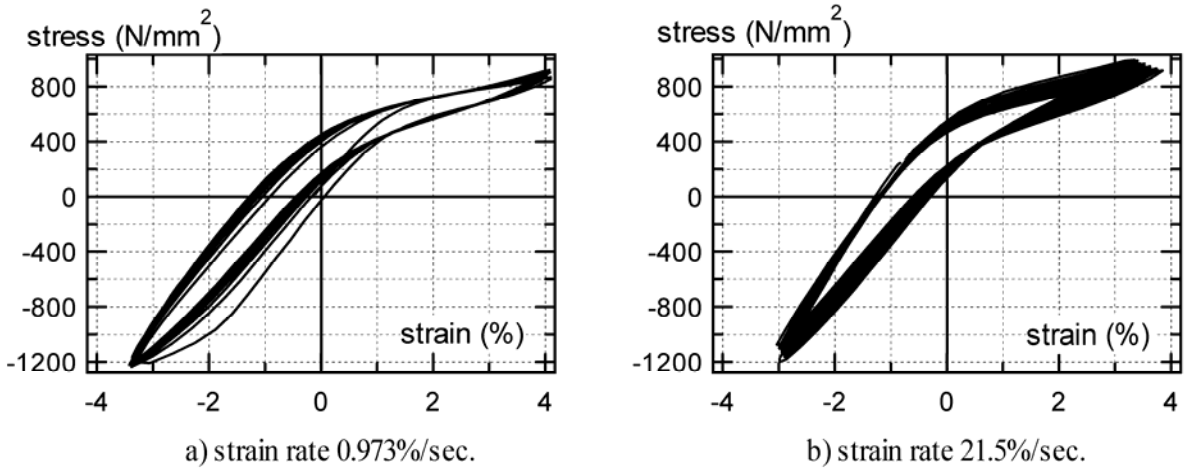


**Figure 5.** Stress-strain relations under dynamic loading

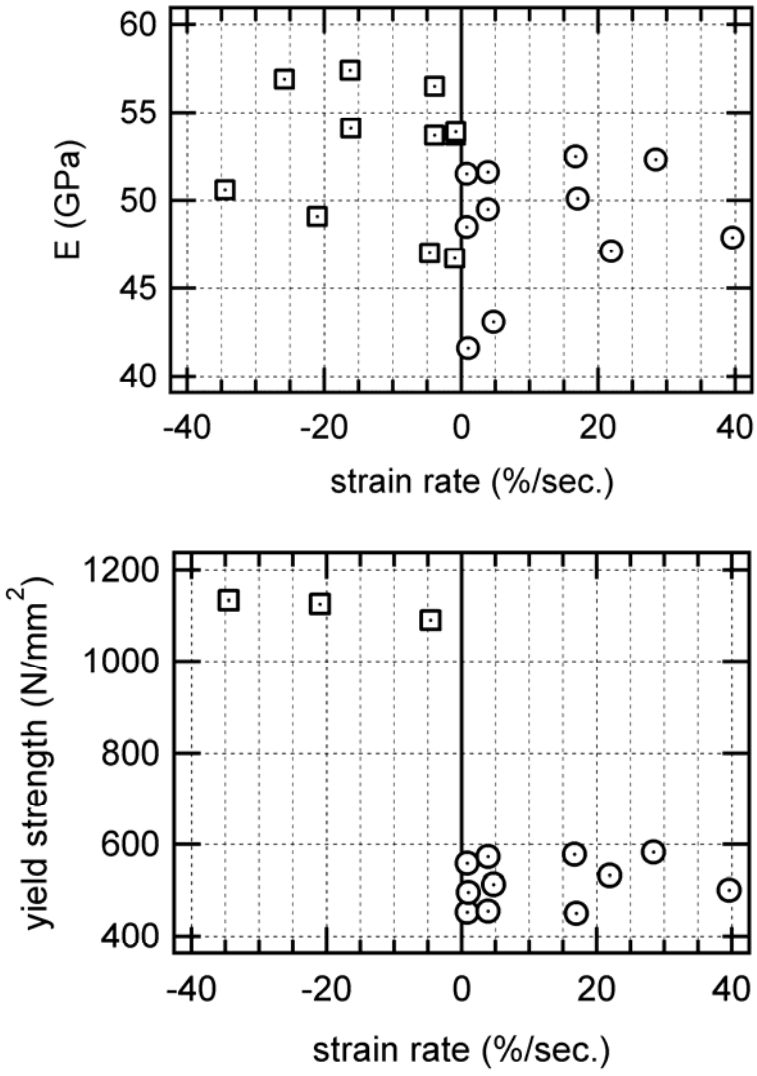


**Figure 6.** Effect of strain rate on Young's modulus & yield strength

Under dynamic loading, the load waveform was triangular. The amplitude was varied at ±1%, ±2%, and ±4%, in that order. Three or four different loading frequencies were used at each amplitude (see Table 1). Ten repetitions were performed for each set of conditions. Therefore, a 110 repeated strain applied to a test specimen. Figure 5 represents results of stress-strain curves under cyclic loading. Overall shapes of curves are similar to those under static loading. Figure 6 presents effects of strain rate on Young's modulus and yield strength defined as 0.2 % offset value. The obvious relation cannot be notified between strain rate and these values. Yield strength in compression is almost two times of tension yielding under the strain rate tested.

### 3. SMA Device for Residential Houses

SMA bars clearly show super-elasticity in tension and not in compression. If SMA bars are used as a tension member, it would effectively control a displacement response of structures and return their lateral drift to zero after earthquakes. Then, a response control device with SMA bars is designed for low-storied houses as the followings: 1) SMA devices carry lateral forces, and beam-to-column frame supports vertical loads, 2) the size of SMA bars is designed so that the device has its required stiffness and strength, 3) SMA bars are effective only in tension. 4) elastic design is applied to the other part of the device under the yield strength of SMA bars (see Figure 7).

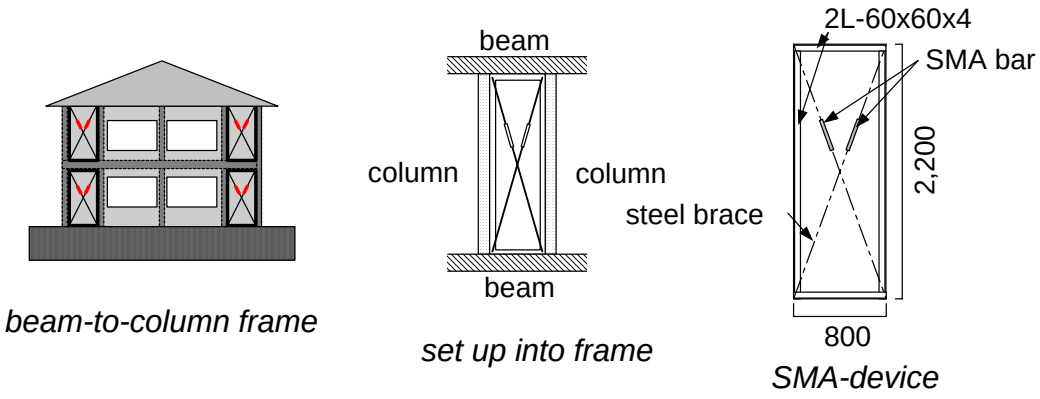


**Figure 7.** SMA device and its set up into a beam-to-column frame

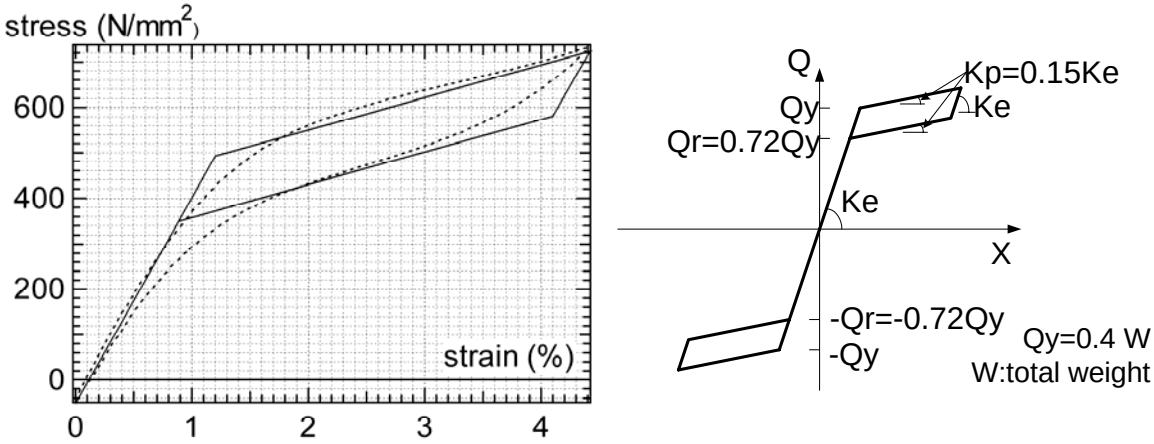


**a)** Stress-strain curve of SMA bars **b)** Restoring characteristic model

**Figure 8.** Restoring characteristic model of a structure with SMA devices

In order to conform the performance of SMA devices under sever earthquakes, the response of a structure with SMA devices was analyzed to El Centro NS wave of 340 gals maximum input. It is assumed that beam-to-column joints of the frame are pin-joint, the frame of the device behaves in elastic and the braces work only in tension. Therefore the restoring force characteristic of the structure can be assumed to be similar to stress-strain curve of SMA, as shown in Figure 8-b). This multi-linear model is based on the material test result of SMA in Figure 8-a). A single degree of freedom model with 0.5 second natural period, 5% viscous damping and lateral yield shear Qy of 40% of total weight was selected as an analytical model, which represents low-storied houses. The response is drawn in Figure 9 in comparison with the system of bi-linear restoring force characteristics. The analysis demonstrates that SMA devices return lateral drift of the structure to zero, on the contrary bi-linear system has some amount of story drift after the quake. But the maximum lateral displacement of the structure with SMA devices is about 1.5 times of the bi-linear model, because of lack of energy dissipation.

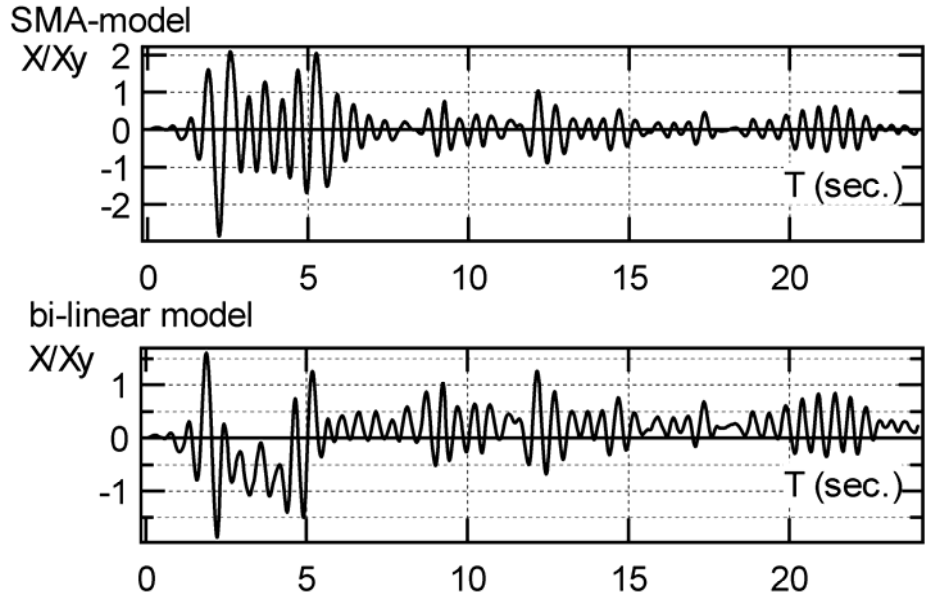


**Figure 9.** Time history of response of SMA-model & bi-linear model

## 4. CONCLUSIONS

This study looked at the stress-strain relationship for a columned specimen of diameter 7 mm taken from a bar of diameter 17 mm. The experiment was conducted with the specimen at the super-elastic alloy phase temperature. The specimen was subjected to static and dynamic compressive and tensile stress. The test results demonstrated that the stress-strain curve for tensile stress is completely different from that for compressive stress, irrespective of whether the load is static or dynamic in nature. Super-elasticity was clearly evident under tensile strain of up to around 5%, but not under compressive strain, due to the presence of residual strain. The yield strength in compression is almost two times of tension yielding under the strain rate tested. SMA devices were designed to control seismic response of wooden houses. Their performance was examined to return story drift of structures to zero after earthquakes, effectively.

## ACKNOWLEDGEMENTS

This study was carried out by the Effector Section (led by University of Tokyo professor Takashi Fujita) of the Super-Intelligent Construction Systems Development project (headed by University of Tokyo professor Shunsuke Otani), a joint research project between Japan and the United States. The authors wish to convey their thanks to all involved.

### REFERENCES

Funakubo T. and et al. (1984) *Shape Memory Alloy.* Sangyotosho, Tokyo

Tamai H. and Kitagawa Y. (2000) Pseudo elastic behavior of shape memory alloy wire and its application to seismic resistance member for building. *Proceedings of the IWCMM10*, Galway, Ireland

*Appendix 2*

*Section 2* *Experimental Study on Torsional Vibration Behavior of Steel Frame Specimen with Eccentricity*

*presented by H.Kato*

*Fifth International Congress on Advances in Civil Engineering, 25-27 September 2002*
*Istanbul Technical University, Istanbul, Turkey*

# Experimental Study on Torsional Vibration Behavior of Steel Frame Specimen with Eccentricity

**Hiroto KATO, Koichi KUSUNOKI**

Department of Structural Engineering, Building Research Institute, Tsukuba, Japan

**Toshibumi FUKUTA**

International Institute of Seismology and Earthquake Engineering,
Building Research Institute, Tsukuba, Japan

**Fumitoshi KUMAZAWA**

Faculty of Engineering, Shibaura Institute of Technology, Tokyo, Japan

## Abstract

Torsional response can destructively effect the seismic capacity of structures. Many damaged buildings due to torsional vibration were observed after sever earthquakes. However, it cannot be said that the mechanism of the damage due to the torsional vibration had been clearly investigated. The main purpose of this paper is to reproduce the torsional response with the pseudo dynamic test technique. One-span, one-bay and two-story steel structures were tested. Three structures that had different eccentric ratios were designed for the pseudo dynamic tests. Furthermore, shaking table tests on three structures were conducted to verify the validity of the pseudo dynamic tests. From the shaking table and the pseudo dynamic tests, it was confirmed that the pseudo dynamic test can adequately reproduce the response of structure with eccentricity; eccentricity was not as effective on the maximum horizontal displacement at center of gravity, but the maximum rotational angle was increased according to its eccentricity.

# 1 Introduction

There have been many buildings damaged due to torsional response during severe earthquakes. However, it cannot be said that the mechanism of the damage due to the torsional response has been clearly investigated. One of the main purposes of this study is to reproduce the torsional response of structures with eccentricity by the pseudo dynamic (PSD) test, and to investigate the mechanism of the damage due to the torsional vibration. In order to verify the validity of the PSD test, the shaking table tests were also conducted (Kato and Kusunoki, 2001). This paper presents the outlines of earthquake response tests and the outcomes from the experimental study.

# 2 Outlines of Specimens

The specimens were one-span, one-bay and two-story steel structures as shown in Fig.1. Rigid slabs made of reinforced concrete provided the inertia force for the shaking table tests, and were used as the loading beam for the PSD test. The weight of each slab was 76.9kN for the first floor and 78.0kN for the second floor. The eccentricity was provided only on the first story by adjusting column positions as shown in Fig.1 a). Two of four columns were located closer to the center of the slab than others. The natural period of the specimens need to be nearly the same to neglect the effects of the frequency characteristics of the input motion. However, it is not easy to provide structures with various stiffness eccentricities that have the same natural period. Therefore the method of adjustment of column positions on the first story mentioned above was applied for the test in order to make the natural periods of test structures almost constant.

H-Shaped steel was used for columns (H-125x125x6.5x9 for the first story and H-100x100x6x8 for the second story). The clear height of column between top and bottom base plates was 1,500mm as shown in Fig. 2. Material test results are shown in Table 1. Table 2 shows the strength of column, the story shear and the story shear coefficients. The story shear coefficient for the first story was 1.43 and 1.85 for the second story.

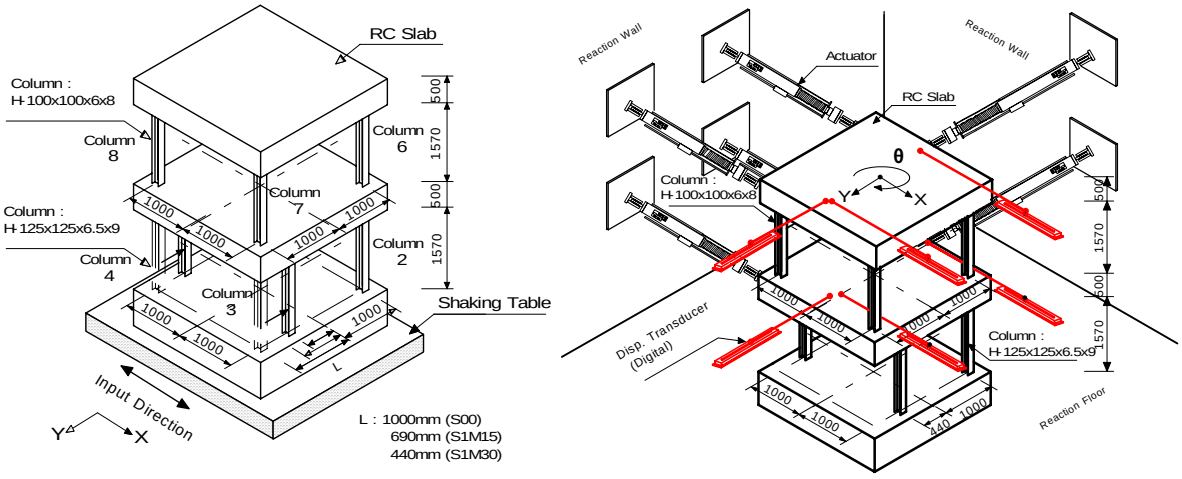


a) Shaking Table Test b) Pseudo Dynamic Test

Fig.1 Setup of Specimen

Table 1 Material Test Results

| | H-125 (First story) | H-100 (Second story) |
|---|---|---|
| Yield Strength (N/mm$^2$) | 304.4/301.7 | 347.8/340.1 |
| Tensile Strength (N/mm$^2$) | 431.9/435.5 | 475.6/473.6 |
| Strain Fracture (%) | 26.4/27.3 | 25.8/25.5 |

Left-side value is for flange, right-side value for web

Table 2 Strength of Specimen

| | Yielding Moment (kN*m) | Story Shear at Yielding (kN) |
|---|---|---|
| First story | 41.4/14.3 [2.9] | 220.8/76.3 (1.43) |
| Second story | 26.6/9.3 [2.9] | 141.9/49.5 (1.85) |

Left-side value is for X Direction, right-side value for Y Direction
[ ] the ratio of yielding moment on X Direction to Y Direction
( ) Story Shear Coefficient

Test parameters are the values of eccentric ratio in the direction of X. The X-axis is the direction of the input motion, as shown in Fig.1 a). The eccentric ratio of 0.0, 0.15 and 0.30 were applied in the X direction. Here, the eccentric ratio is defined as a function of distance between center of gravity and rigidity (Eq.1), which is prescribed in the Building Standard Low Enforcement Order of Japan, and represents how easily a structure can vibrate torsionaly (JBC/Japan Building Center, 2001).

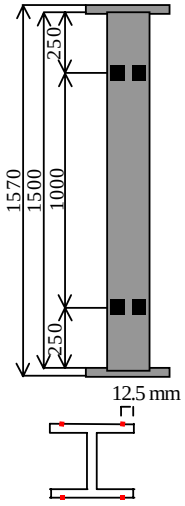

Fig. 2 Column

$$R_e = \frac{e}{r_e} \qquad (1)$$

e : Eccentric Distance. The distance between center of gravity and rigidity

$r_e$ : Radius of Spring Force.

$$r_{ex} = \sqrt{K_R / K_x}\ ,\quad r_{ey} = \sqrt{K_R / K_y}$$

$K_R$ : Torsional Stiffness.

$K_x$, $K_y$ : Horizontal Stiffness to The Direction of X and Y

In structural design of building with eccentric ration larger than 0.15, design external force should be made to increase up to 1.5 times in accordance with the values of eccentric ratio. An eccentric ratio of zero means that the structure has no eccentricity. The test parameters are shown in Table 3. The number of specimens are six, three were prepared for the PSD tests (P00, P1M15 and P1M30).In addition, three specimens (S00, S1M15 and S1M30) were used for the shaking table tests in order to compare the reproduced behaviors between the PSD test and those of the shaking table tests. In order to achieve the specific eccentricity, columns were shifted by the distance shown in Table 3 from the location for the structure without eccentricity.

The test structure was assumed to be 1/2 scaled model of a real size structure. However, no prototype structure in real size was designed because the main purpose of this research was to

investigate the basic effect of the torsional response on structural damages, not to observe the response of a specific structure. Because of this, the horizontal strength of column was assumed simply to be proportional to the area of section. Scale factors for each item are listed in Table 4 (Kumazawa, 1996). Single underlined items are the items that cannot be scaled down, and double underlined items are the items of which scale factor does not have proper relationship with the real size structure.

Table 3 Names of Specimens and Test Parameters

| | | Shifted Distance from Uniform Arrange (mm) | Names of Specimens | |
|---|---|---|---|---|
| | | | Shaking Table Test | Pseudo Dynamic Test |
| Eccentric Ratio in X direction | 0.00 | 0 | S00 | P00 |
| | 0.15 | 310 | S1M15 | P1M15 |
| | 0.30 | 560 | S1M30 | P1M30 |

Table 4 Scale Factors

| Physical Phenomena | | | |
|---|---|---|---|
| Length | 1/2 | Area | 1/4 |
| Volume | 1/8 | Gravity Acceleration | 1.0 |
| Specific gravity | 1.0 | Mass | 1/8 |
| Rotational inertia | 1/32 | Time | 1/2 |
| **Column** | | | |
| Young's modulus | 1.0 | Axial strain | 1.0 |
| Curvature | 2.0 | Twisting strain | 2.0 |
| Horizontal strength | 1/4 | Horizontal stiffness | 1/2 |
| Yield deformation | 1/2 | Rotational stiffness | 1/8 |
| **Response of Structure** | | | |
| Natural period | 1/2 | Horizontal acceleration | 2.0 |
| Horizontal velocity | 1.0 | Horizontal deformation | 1/2 |
| Rotational acceleration | 1.0 | Rotational velocity | 1.0 |
| Rotational deformation | 1.0 | | |

Strains of steel columns were measured with strain gauges put on the flange at both ends of columns as shown in Fig. 2 (black rectangular marks show strain gauge locations). Four strain gauges were put at one end, eight gauges were used for one column, and totally strains at 64 different points were measured during the PSD and the shaking table tests.

Three displacement transducers were used to measure response bi-directional horizontal displacement and rotational angle of each floor as shown in Fig.1 b). Two transducers were for X-direction and rotation, and one was for Y-direction. Two additional transducers were used to measure slip displacement at bottom of basement during the shaking table tests.

Three accelerometers were used to measure response acceleration during each floor at the shaking table test. Two were for Y-direction and rotation, and one was for X-direction. One accelerometer was placed on the center of the basement to measure actual input motion to a specimen.

# 3 Input Motions

The North-South component of JMA-Kobe (Kobe Observatory of Japan Meteorological Agency) recorded at the Hyogo-Ken-Nanbu earthquake in 1995 was used for the input motion, of which time axis was scaled down by 1/2 according to the scale factor. The input earthquake wave and the response acceleration magnification with various damping coefficient are shown in Fig.3. Five different normalized peak acceleration waves of 200, 450, 900, 1640 and 2400cm/sec$^2$ were inputted in order of level. Peak accelerations in a real size are 100, 225, 400, 820 and 1200 cm/sec$^2$ because of scale factors. The shaking table tests were conducted with these input motions prior to the PSD tests, and recorded acceleration at the basement of each specimen was used for the input motion to the PSD tests.

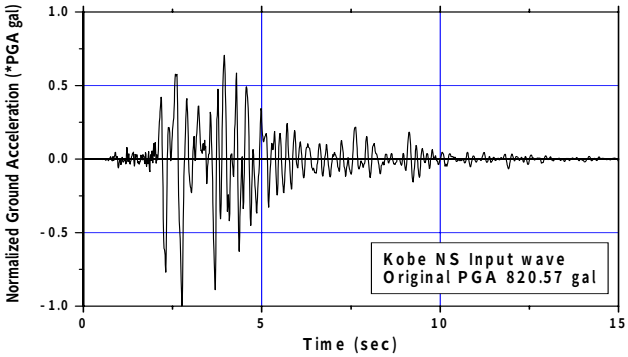


a) Earthquake Acceleration

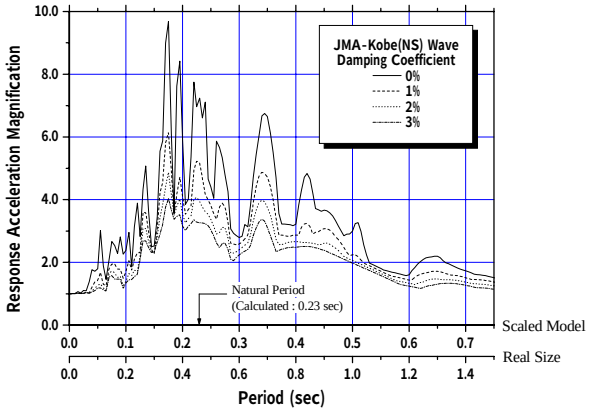


b) Response Acceleration Magnification

Fig. 3 Input Acceleration Wave

# 4 Test Results and Discussions

## 4.1 Fundamental Characteristics of Specimens

In order to measure natural periods and damping coefficients of specimens, responses with the white noise input were measured at the shaking table tests. On the other hand, since a stiffness matrix was needed for the PSD tests to assume a damping matrix, unit loading tests, that small amount of force was loaded at each floor and in each direction, were carried out just after setting up each specimen. Then, all responses for each force were measured, and the flexibility matrix was generated. The natural periods were calculated with the flexibility matrix and the mass matrix for each specimen. Measured natural periods were listed in Table 5. The damping coefficients could be assumed as 1% from the shaking table test with the white noise. The damping coefficients of 1% proportional to the initial stiffness were assumed for the PSD tests.

The natural periods in both X and Y direction of the shaking table and the PSD tests are almost the same, however, those of torsional response are a little different. Since the natural periods of the shaking table tests were calculated with transfer function at the white noise input, the accuracy of the natural period of the torsional response is not so high because it is higher modes.

Table 5 Natural Periods (sec)

| Specimen | X Direction | Y Direction | Torsion |
|---|---|---|---|
| P00 | 0.264 | 0.401 | 0.201 |
| P1M15 | 0.264 | 0.390 | 0.217 |
| P1M30 | 0.276 | 0.393 | 0.226 |
| S00 | 0.260 | 0.410 | 0.220 |
| S1M15 | 0.280 | 0.410 | 0.240 |
| S1M30 | 0.280 | 0.410 | 0.250 |

### 4.2 Comparison of Results of PSD Tests and Shaking Table Tests

**Responses of Specimens**

The response displacements at center of gravity on roof floor in the X direction and rotational angles of the first story of which the input level was 1640cm/sec$^2$, are shown in Fig.4. In the figure, solid lines show the results of the PSD tests and broken lines are those of the shaking table tests. It can be said that the response displacements of P1M15 and P1M30 agreed very well with those of the shaking table tests, which include maximum response displacements. And the rotational angles of those specimens also show rather well correspondence. However, the response displacement of P00 was evidently larger than that of S00, the behaviors of both did not coincide. From Fig. 4, the maximum response displacements at center of gravity of employed specimens are almost in agreement, in spite of difference of eccentric ratios. Meanwhile the response rotational angles of specimens with eccentricity grow with increasing of eccentric ratio, as against those of P00 and S00 are very small. It was observed that the eccentricity of specimen was inclined to have an influence on the rotational response.

The relationship between story shear force and inter-story drift in the first story of the PSD for the same input level are compared with those of the shaking table tests in Fig.5. Though the behaviors of P1M15 and P1M30 agreed well with those of the shaking table tests, the result of P00 was different from that of S00, especially the initial stiffness of the shaking table test was a little higher than that of the PSD test. Because of the difference of stiffness, the response of the PSD test did not agree with that of the shaking table test. The reason why the stiffness of S00 and P00 were different needs further investigation. From these results, it will be said that the PSD test can adequately reproduce the dynamic response of specimen, if the stiffness of specimen is in agreement.

The orbits at center of gravity in the first story of the PSD tests are illustrated in Fig.6. The results of P1M15 and P1M30 show drifts in Y direction, it is understood that the effects of eccentricity promote the deflection of perpendicular direction where input motions were not given.

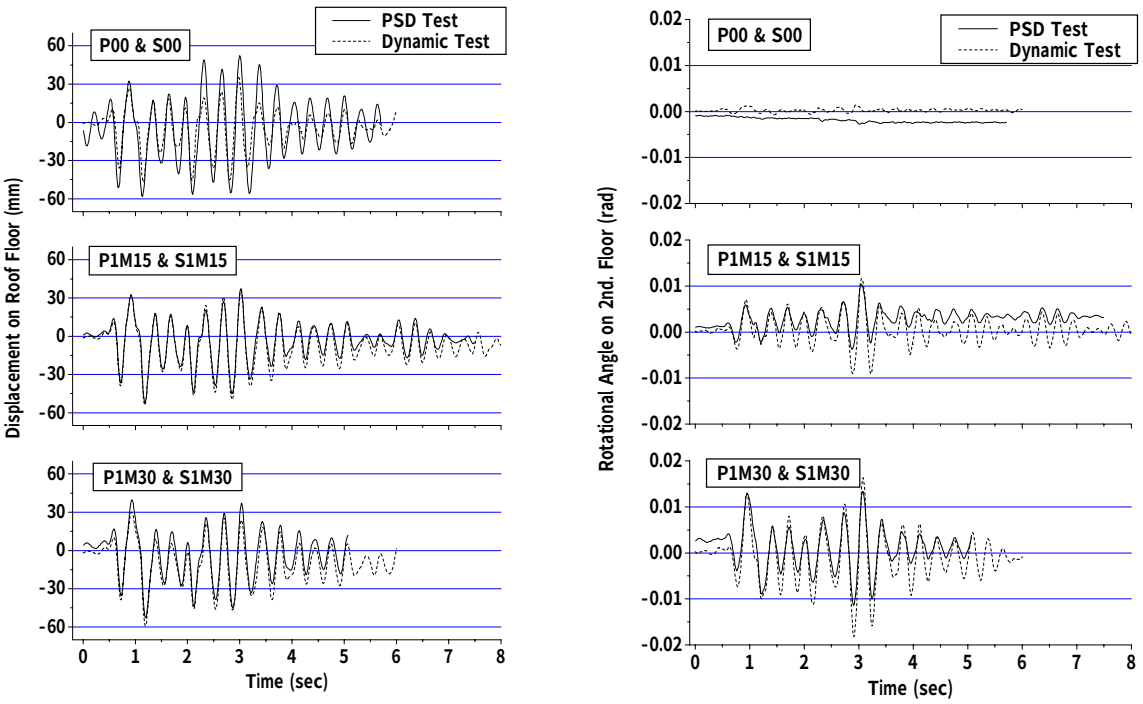


a) Displacement Responses (Roof Floor) b) Rotational Angle Responses (First Story)

Fig.4 Dynamic Responses of Specimens for 1640cm/sec$^2$ Input

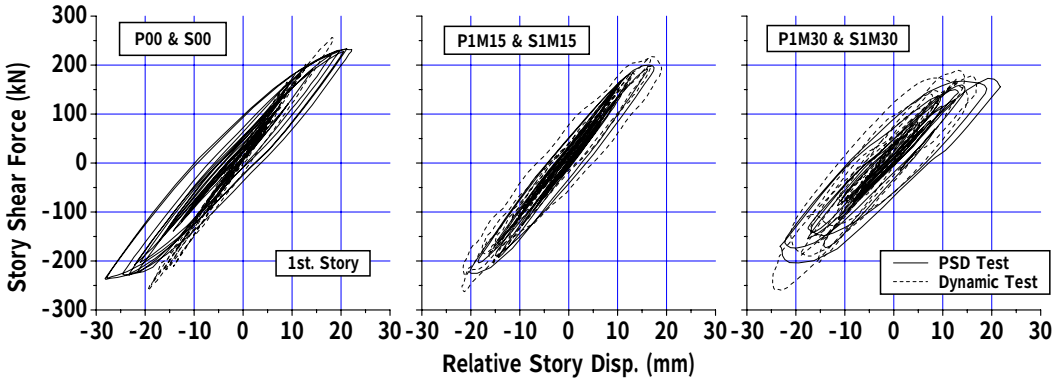


Fig.5 Story Shear Force and Story Drift Relationship (1640cm/sec$^2$ Input)

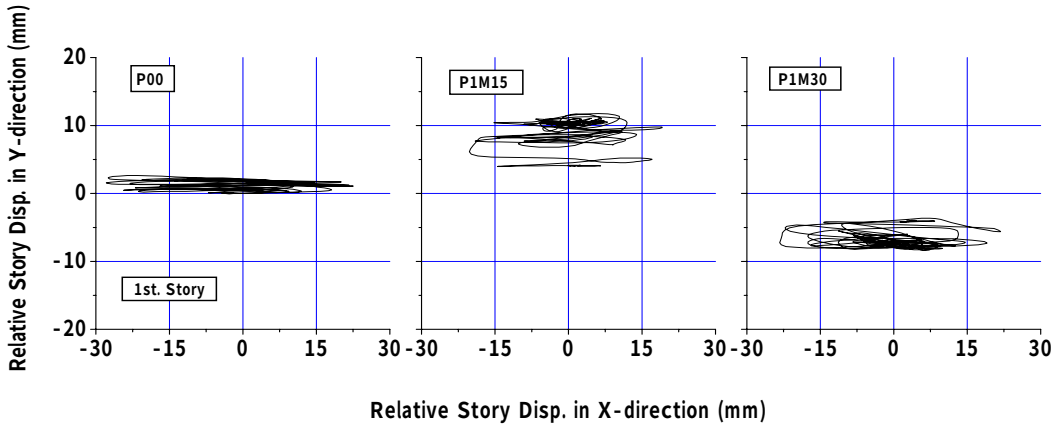


Fig.6 Orbits of Center of Gravity of PSD Specimens (1640cm/sec$^2$ Input)

**Maximum Responses**

Figure 7 a) shows maximum response displacements at center of gravity of the first story in the X direction for each input level. As mentioned before, P00 and S00 are quite different especially for relatively large input levels. P1M15 and P1M30 agree well with S1M15 and S1M30 regardless of input level. It can be seen that there is the tendency to slightly increase the maximum response displacement at center of gravity with increasing of the eccentric ratio. Figure 7 b) shows maximum torsional response angle of the first story for each input level. Maximum torsional response angle of P1M30 at input level of 1640 cm/sec$^2$ was 28% smaller than that of S1M30. Maximum torsional response angle is the relative angle to the basement and residual torsional angle could be accumulated. Maximum angle of P1M30 at input level of 2400 cm/sec$^2$ was also 27% smaller than that of S1M30. Maximum torsional response angle increased according to the eccentric ratio. For example, the ratios of maximum angle to P1M15 at input level of 1640 cm/sec$^2$ were 1.15 (P1M30).

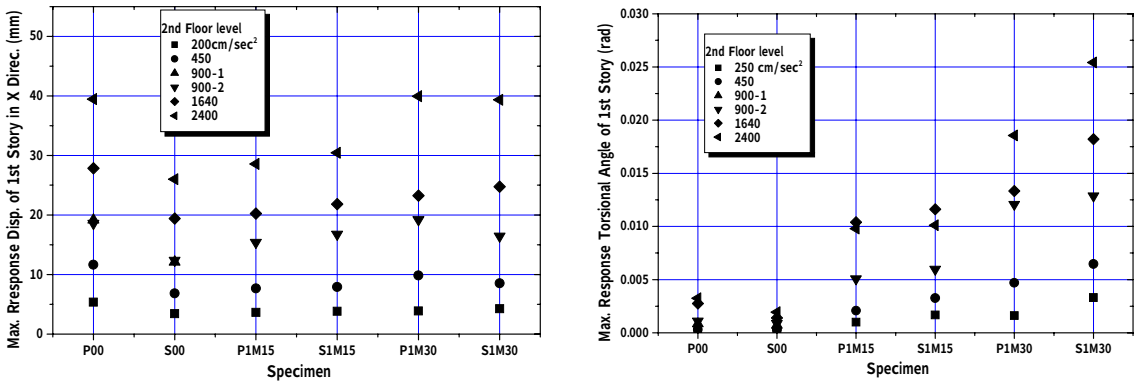


a) Disp. of 1st Story b) Torsional Angle of 1st Story

Fig.7 Maximum Responses (1640cm/sec$^2$ Input)

**Responses of Individual Columns**

Since the tendency of promoting torsional vibration by eccentricity of specimen was observed as mentioned above, the responses of individual columns will be indicated below. Figure 8 shows the response displacement of eccentric and non-eccentric bays with those at center of gravity of P1M30 at input level of 1640 cm/sec$^2$. The displacement of eccentric bay are larger than that of center of gravity, on the other hand the one of non-eccentric bay show opposite trend. The ratio of maximum response of eccentric bay to that at center of gravity was about 1.4; the one of non-eccentric bay was 0.6. Those outcomes make clear that the eccentric bay is forced to be deformed largely, in spite of the displacements at center of gravity of each specimens were not so different as shown in Fig.4 a).

The restoring characteristics of individual columns in the first story of specimens with eccentricity are illustrated in Fig.9. Here, Column 2 is in non-eccentric bay and Column 3 is in eccentric bay as shown in Fig.1 a). The abscissa of the graph is deformation of column and the ordinate shows shear force obtained from measured strain of column. The restoring characteristics of the PSD and the shaking table tests adequately agreed with each other, it is

conformed that the both results correspond in the level of structural elements. The Columns 3 have a spindle-shaped hysteresis loops, it means that the columns had been yield and reached in plastic range. On the other hand, the Columns 2 show elastic restoring characteristics, those had remained in elastic range. The phenomena which areas of hysteresis loops of P1M30 and S1M30 are larger than those of P1M15 and S1M15, show the possibility that structural element in eccentric bay will be suffered heavy damage in large earthquake excitations.

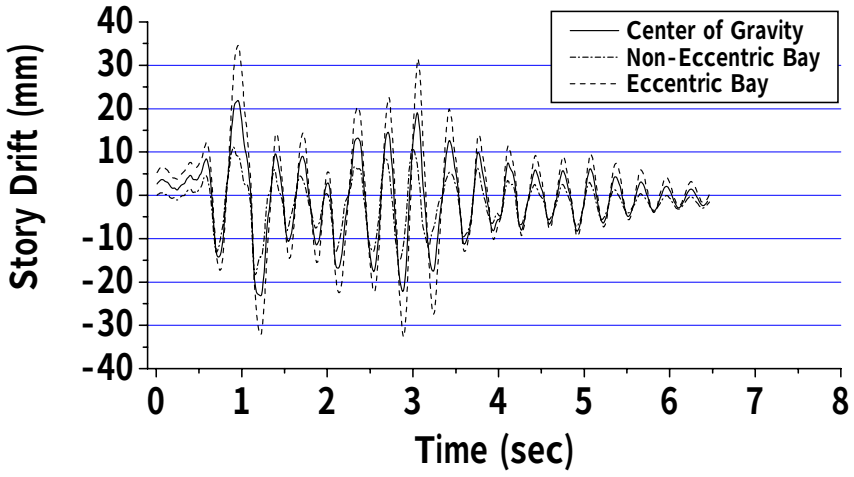


Fig.8 Comparison of Displacement Response in Each Streets of Specimen
(1st story of P1M30, 1640cm/sec$^2$ Input)

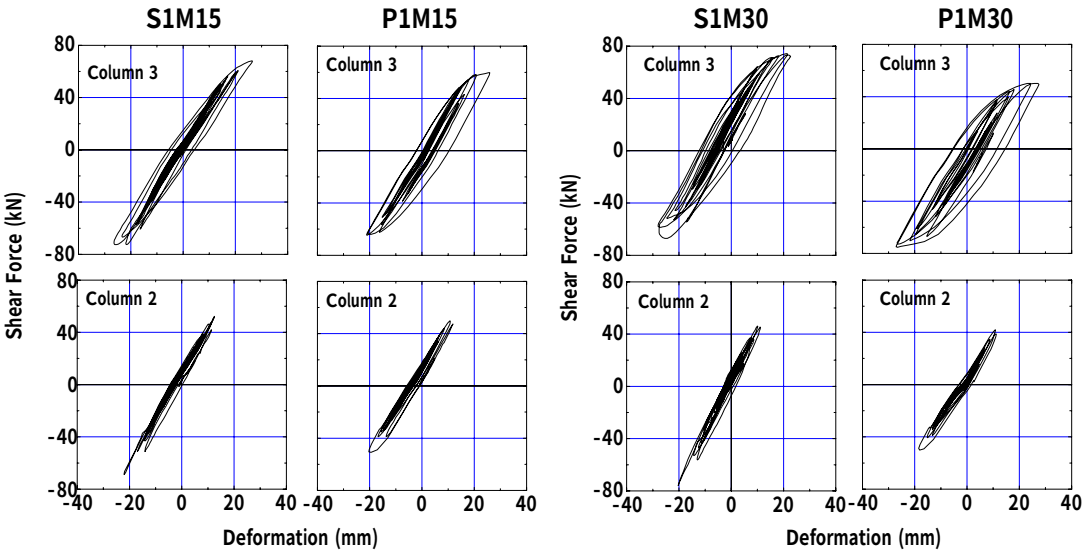


a) Eccentric Ratio 0.15 b) Eccentric Ratio 0.30

Fig.9 Restoring Characteristics of Individual Columns (1640cm/sec$^2$ Input)

## 5 Concluding Remarks

In order to investigate the mechanism of damage due to torsional response, a series of PSD tests on the specimens with eccentricity were conducted. Furthermore, in order to verify the validity of the PSD test, the shaking table tests on the same specimens were conducted. The outcomes from this experimental study are summarized as follows;

1. The pseudo dynamic test technique with torsional response was newly developed. If the stiffness of specimen can be given properly, the pseudo dynamic test can reproduce the dynamic response of eccentric specimen with sufficient accuracy.
2. The displacement response at center of gravity of specimens was not so influenced by the values of eccentric ratio.
3. Torsional response angle increases evidently according to the eccentric ratio.
4. There is the possibility that structural elements in eccentric bay will be suffered heavy damage in large earthquake excitations.

## Acknowledgement

The authors express their appreciation to Messrs Yuuichi Hirosaki (graduate student in Shibaura Institute of Technology), Kenji Ashida (Nohara Co. Ltd.), Isao Fujimoto, Yasuhiro Kiuchi and Yutaka Komatsu (The Center for Better Living) for their contribution to conduct this experimental research.

## References

JBC/Japan Building Center (2001). Guideline for Technical Standard Related to Building Structure, (in Japanese)

Kato H. and Kusunoki K., et al. (2001). Study on earthquake response characteristics of frame structures with eccentricity (Part 1– 3). Summaries of Technical Papers of AIJ Annual Meeting, (in Japanese)

Kumazawa F. (1996). Study on Response Characteristics of Small Scaled Reinforced Concrete Structures. Ph. D Thesis, University of Tokyo (in Japanese)

*Appendix 3*

*Section 3* *Seismic Performance of Retrofitted RC Slab Connected with Strengthening Frame*

*presented by M.Inukai*

# SEISMIC PERFORMANCE OF RETROFITTED RC SLAB CONNECTED WITH STRENGTHENING FRAME

Mizuo INUKAI[1], Takashi KAMINOSONO[2]
Motoyuki TOHARA[3], Tadashi KIMURA[3], Hironobu IMAMURA[3]

Key Words: 1995 Hyogoken Nanbu Earthquake, new retrofit method, existing building, reinforced concrete slab, non-shrinkage mortar, apartment house

## 1. Purpose

Since the 1995 Hyogoken Nanbu Earthquake, the retrofits for the old buildings are done but there are few research activities about the retrofit method for middle high rise apartment houses. Generally, the retrofit is executed for office buildings, school buildings and so on which the users can move out during the retrofit construction works.

It means that it is needed to develop a new retrofit method which the resident people can use their buildings continuously during this retrofit works. In apartment houses, there are always few residents who cannot accept the temporary remove during retrofit construction works.

In 1998, the research activities was done about the retrofit of the high rise apartment house with Steel Reinforced Concreter Structure which was designed by the old seismic code before 1981. These activities proposed that the retrofit method should use the strengthening frame with Reinforced Concrete Structure outside of the existing structure [1]. And the researches were not made about the construction method for the continuous use or the connecting method between the existing structure and the strengthening frame.

Therefore, this research paper describes the experimental study about the seismic performance of the reinforced concrete slabs retrofitted by the non-shrinkage mortar. This slab is connected between the existing reinforced concrete frame structure and the strengthening frame.

## 2. Model building

The model building is 11 storeys apartment house [1]. The lower 7 storeys is the Steel Reinforced Concrete Structure, and the upper than it is the Reinforced Concrete Structure. The number of spans in the span direction (X-direction) is 1 and one in the ridge direction (Y-direction) is 14 (Fig.1, Table 1). This model building was designed by the old seismic code before 1981. According to the seismicity assessment [1], the maximum *Is* index [2] on each floor was from 03. to 0.8, and especially the maximum *Is* index on 5-10 floor was less than 0.6. That means the building needs some retrofit.

Table 1 Model Building

| | |
|---|---|
| Size | 11 storeys with pent house of 3 storeys |
| Structure type | -Steel Reinforced Concrete<br>(Lower than 1 meter high on 7th floor)<br>-Reinforced Concrete (Upper than it) |
| Material | -Concrete<br>(Compressive strength: 20(N/mm$^2$))<br>(Lower than floor beam on 3rd floor)<br>-Light Concrete<br>(Compressive strength 20(N/mm$^2$))<br>(Upper than column on 3rd floor)<br>-Steel bars: SR235,SD295,SD345<br>-Steel: SS400 |

1) Senior Research Engineer, Building Department, National Institute for Land and Infrastructure Management, Ministry of Land, Infrastructure and Transport. Tsukuba-shi, Ibaraki-ken, 305-0802, Japan)
2)Associate Director, ditto.
3)Urban Development Corporation

The retrofit plan in 1998 proposed the required strength to get the enough *Is* index which is more than 0.6. And the retrofit method should use the strengthening frame on the outside of the corridor and the verandah of the building by connecting with the existing structure using prestress steel bars. This strengthening frame should have 7 spans among the 14 spans and the existing slab in 3 spans should be retrofitted by the RC slab. The problem of this method is that almost reinforce concrete slabs should be retrofitted for their shear force transfer performance between strengthening frames beside the outside frames. The strengthening frame is designed to support the strength shortage of the existing frames. This shortage of strength should be transferred from the existing frames to strengthening frames finally to foundations or ground.

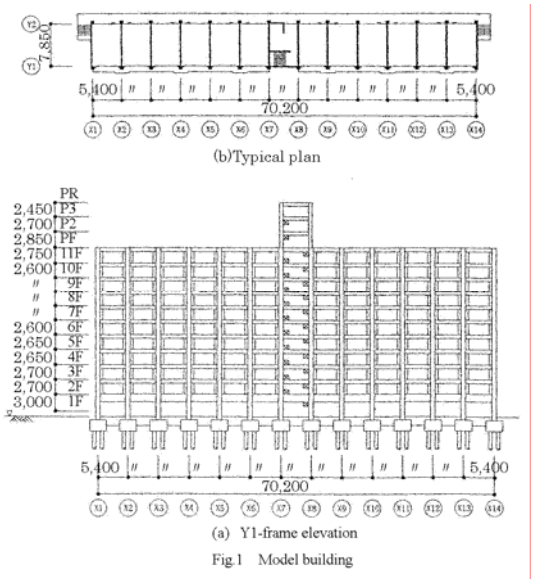

Fig.1 Model building

The existing slabs of this building are cantilever with beams at their end.

In this research paper, we used the Anchors to set up the retrofit slabs underneath the existing slabs. That is because the Anchors don't need the construction workers to enter into some private spaces without any anchorage wholes which go through the beams. This retrofit construction works need only the public spaces, for example, corridor, or verandah. So, it is useful to build strengthening frames beside the outside frames.

In order to decrease the period of the construction works, we use half-precast slabs for the retrofit slabs. And we considered that the columns of the strengthening frame should be precast RC members and the beams should be cast-in-place RC members. That is because the beams of the strengthening frame need some large tolerance about the position of the anchorage wholes to connect with the existing members which do not have enough accuracy about the position of the steel bars. We used half-precast slabs because we can shorten the formworks in the public spaces which sometimes interrupt the walks or the emergency escapes for residents (Fig. 2).

Therefore, it is possible to use continuously the apartment house during the retrofit construction works. And we need the experiments about this retrofit method and its seismic property.

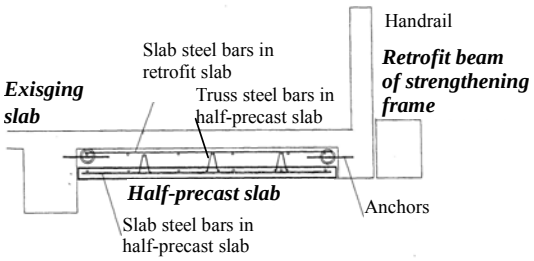

Section of corridor in public space

Fig.2 Overview of Retrofit slab

## 3. Specimens

The specimens are shown in Table 2 and Fig.3. The specimens are made of existing slab in depth of 110mm and retrofit slab in depth of 100mm which is cast by non-shrinkage mortar which is between existing slab and half-precast slab in depth of

Table2 Specimens (unit:mm)

| Specimen | Size | Existing Slab | Retrofit Slab | | Half-Precast Slab | |
|---|---|---|---|---|---|---|
| Flret-0m (no-retrofitted) | Full-scale Slab | Length:2,000<br>Width :1,300<br>Depth : 110<br>Slab steel bar 1 (Span-direction) D13@200 double<br>Slab steel bar 2 (Ridge-direction) D10@200 double | — | | — | |
| Flret-1m (retrofitted) | | | Length 1,000 | Width:1,300<br>Depth: 100<br>Slab Steel bar (Both directions) D10@200<br>Anchors D16@200<br>Insert depth: 130<br>Whole diameter:20<br>Anchorage length: 480 | Length 1,000 | Width:1,260<br>Depth: 60<br>Slab steel bar (Both directions) D10@200 double<br>Truss steel bar ϕ13-ϕ6-ϕ6-H65 |
| Flret-2m (retrofitted) | | | Length 2,000 | | Length 2,000 | |

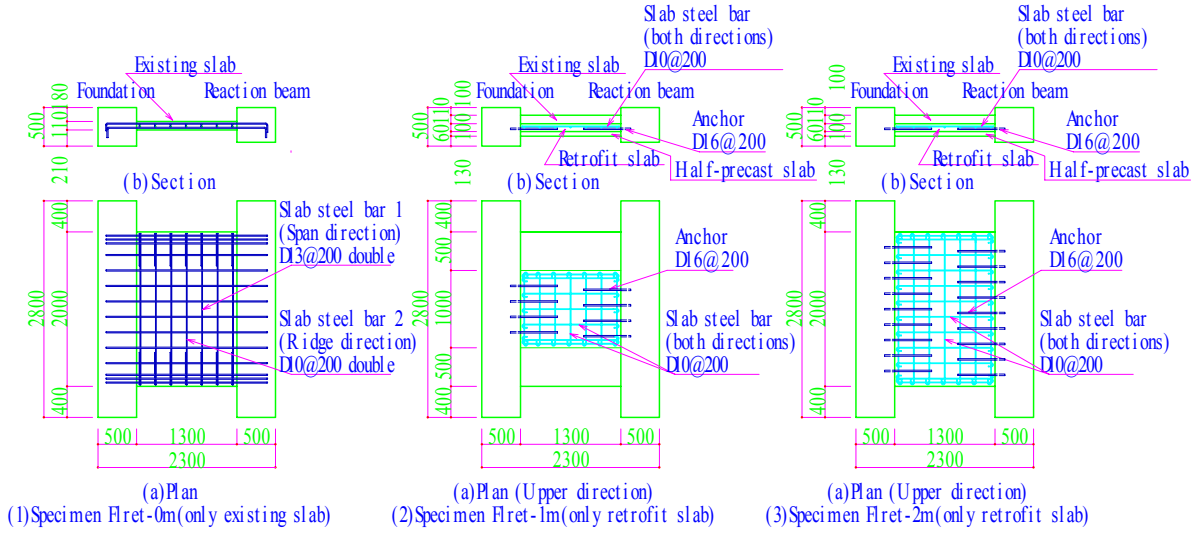


Fig.3 Steel bar arrangement

60mm. The half-precast slab has a function to be forms for fresh concrete. The total depth of these specimens is 270 mm which is the same as the depth of the beams at the end of the existing slabs. The scale is full-scale because we have to use the drill machine for anchors underneath the existing slabs. The minimum size between the bottom end of the existing slab and the center of anchors is 65mm.

In order to assess the effect of the retrofit and the length of retrofit slabs, the parameter of the specimens is the length of retrofit slab which is 0m, 1m and 2m.

The existing slab has steel bars D10@200double in the ridge direction (Y-direction) and D13@200double in the span direction (X-direction). In the model building, slab steel bar is D10@200double in both directions. The existing slab steel bars are increased because we considered that the specimens should be collapsed in shear mode and should have some effect of the next existing slab in the ridge direction.

As for the making of the specimen with retrofit slab, at first, we made a existing slab, a reaction beam and a foundation. 1 week later, we cast a retrofit slab after the cast of anchors D16@200 on the reaction beam and the foundation underneath the existing slab, retrofit slab steel bars D10@200 in both directions, half-precast slab with a truss of round steel bars of ϕ13-ϕ6-ϕ6 and which height is 65mm, and non-shrinkage mortar between the existing slab and the half-precast slab.

When anchors are cast, anchorage wholes in depth of 130mm and in diameter of

20mm are prepared before the casting of concrete in the foundation and the reaction beam. The anchorage material for D16@200 is the capsule type adhesives made of glass tube. One tube is inserted into the anchorage whole, and an anchor steel bar D16 with a section end 45 degrees cut is inserted into an anchorage whole with rotations by a drill machine. The anchorage length from the surface of the foundation or the beam to the other end of anchors D16 is 480mm. We used a low noise drill machine for the residents of the apartment house.

The diameter of anchor 16mm is the maximum size which is possible to cast under the corridor slab in width of 1,300mm because the required anchorage length is 30 x diameter (=480mm), the required insert length is 130mm, and the length of a drill machine is about 400mm. Total length is just less than 1,300mm. The space between anchors 200mm is the required minimum size.

Non-shrinkage mortar should be filled in all volume of the retrofit slab. That is why we made a filling test before casting which is executed by the Prestressed Concrete Construction Company (Photo 1). The wooden forms for the 4 headers and the bottom, and the acrylic plate for the top were prepared for the filling test. The vinyl tubes are inserted from the one end of this filling test specimen to the opposite end, and non-shrinkage mortar is cast from the opposite end. The vinyl tubes inserted in the opposite end is the air exit for filling. After the mortar reached the one end, the specimen is left for cure in one day. The next day, we confirmed that the mortar is filled enough just underneath the acrylic plate.

The material properties are shown in Table 3 and Table 4.

Table3 Material properties of Concrete and Mortar

| Part to be used | σc | Ec | εc |
|---|---|---|---|
| Concrete of slab in not-retrofitted specimen | 31.3 | 3.33 | 1,775 |
| Concrete of existing slab in retrofitted specimens | 33.5 | 3.07 | 1,943 |
| Mortar of retrofit slab | 60.1 | 2.17 | 5,411 |
| Concrete of half-precast slab | 40.6 | 2.80 | 2,248 |

Notes) σc: Compressive strength(N/mm$^2$)
Ec: Young modulus x10$^4$(N/mm$^2$)
εc: Strain at compressive strength x10$^{-6}$(mm/mm)

Table 4 Material properties of Steel bars and Anchors

| Part to be used | Size (Nominal name) | σt | Es | εs | σo |
|---|---|---|---|---|---|
| Existing slab | D13(SD295A) | 349 | 1.79 | 1,951 | 493 |
| | D10(SD295A) | 338 | 1.79 | 1,889 | 468 |
| Retrofit slab | D10(SD295A) | 361 | 1.75 | 2,060 | 505 |
| Anchor | D16(SD295A) | 343 | 1.81 | 1,892 | 484 |

Notes) σt: Yield strength(N/mm$^2$)
Es: Young modulus x10$^5$(N/mm$^2$)
εs: Strain at yielding x10$^{-6}$(mm/mm)
σo: Tensile strength(N/mm$^2$)

Photo 1 Filling test of non-shrinkage mortar

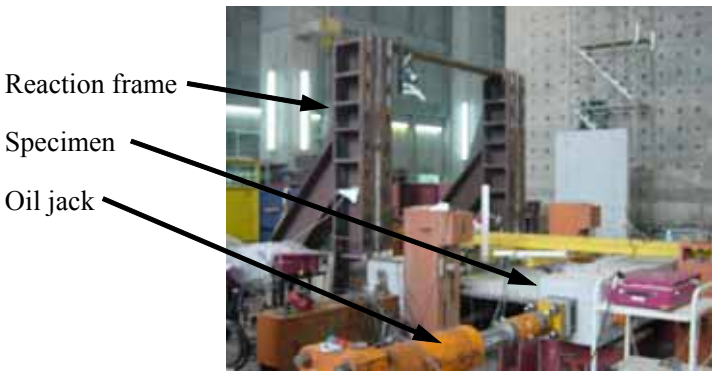


Photo 2 Loading test

## 4. Experiment

The loading test is made with the slab horizontal (Photo 2). By this loading

test, we can know that the retrofit slab or the half-precast slab would fall down or not.

The foundation is fixed to the reaction floor and the reaction frame, and the reaction beam is supported by the roller supports. 2 oil jacks on the 2 ends of the reaction beam load the horizontal force in plane of a slab like a cantilever beam loading.

During the loading, when the slab steel bar in the span direction is yielding, another prestress steel bars are installed near the ends of the slab to escape from the flexural failure mode.

## 5. Results

The horizontal force – displacement relationship is shown Fig.4. The maximum horizontal force is 913kN of specimen Flret-0m, 1,037kN of Flret-1m, and 1,341kN of Flret-2m. The failure mode is shear failure for all of 3 specimens.

As for the retrofitted specimens, Flret-1m and Flret-2m, the retrofit slab is separated from the existing slab at the displacement more than 20mm and do not fall down to the ground.

As for the specimen Flret-1m, in the half-precast slab, many flexural cracks and shear cracks take place. At the foundation, the same crack as the cone failure of anchors take place.

As for the specimen Flret-2m, in the half-precast slab, any cracks do not take place.

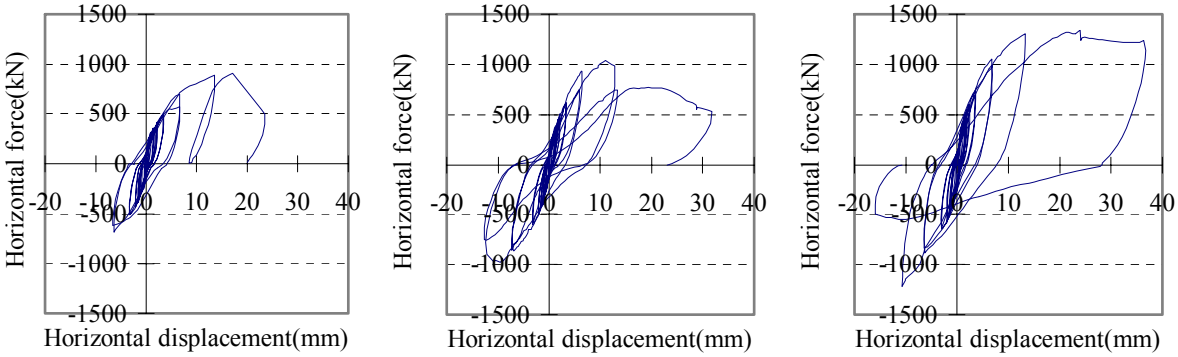


(1)Specimen Flret-0m (2)Specimen Flret-1m (3)Specimen Flret-2m

Fig.4 Horizontal force – displacement Relationship

## 6. Conclusions

(1) These specimens make clear that the shear force transfer property between the strengthening frame and the outside frame increases by the set up of the retrofit slab and the length of the retrofit slab.

(2) .It is possible to cast the retrofit slab underneath the existing slab with the enough filling property.

(3) By the anchors and the half-precast slabs, it is possible to use the building continuously during retrofit works.

**[Reference]**

[1] ”Research Report about the Development of Retrofit Techniques for Apartment Houses”, Housing and Urban Development Corporation, etc., March 1999, pp.184-226. (in Japanese)

[2] “Damage Classification Method for Damaged Buildings Post-Earthquake and Seismic Retrofit Guideline”, The Japan Building Disaster Prevention Association, Sept.2001. (in Japanese)